



Gated-controlled electron pumping in connected quantum rings



R.P.A. Lima^{a,*}, F. Domínguez-Adame^b

^a GISC and GFTC, Instituto de Física, Universidade Federal de Alagoas, Maceió, AL 57072-970, Brazil

^b GISC, Departamento de Física de Materiales, Universidad Complutense, E-28040 Madrid, Spain

ARTICLE INFO

Article history:

Received 28 April 2014

Received in revised form 11 June 2014

Accepted 25 June 2014

Available online 1 July 2014

Communicated by V. Markel

Keywords:

Quantum pump

Quantum ring

Time-dependent scattering

ABSTRACT

We study the electronic transport across connected quantum rings attached to leads and subjected to time-harmonic side-gate voltages. Using the Floquet formalism, we calculate the net pumped current generated and controlled by the side-gate voltage. The control of the current is achieved by varying the phase shift between the two side-gate voltages as well as the Fermi energy. In particular, the maximum current is reached when the side-gate voltages are in quadrature. This new design based on connected quantum rings controlled without magnetic fields can be easily integrated in standard electronic devices.

© 2014 Elsevier B.V. All rights reserved.

1. Introduction

Recently developed nanofabrication of quantum rings and dots by self-assembling [1–4], lithographic [5,6] or etching techniques [7] has opened an active area of research, both theoretical and experimental. Due to their high crystalline quality, the coherence length in these nanostructures is in the micron scale, usually larger than their size, and then electron transport is ballistic [8]. As a consequence, quantum effects, such as quantum interference, play a major role in the design of future nanodevices based on quantum dots and rings. A cornerstone of coherent electron transport and the subsequent interference effects in mesoscopic rings is the celebrated Aharonov–Bohm (AB) effect [9]. Electrons passing through the two arms accumulate a phase difference due to the magnetic flux threading the ring. The resulting interference pattern leads to a modulation of the conductance as a function of the magnetic flux. The predicted phase shift was indeed soon confirmed experimentally [10]. Remarkably, even excitons can undergo AB oscillations [11–15], in spite of being neutral entities.

The combination of two different quantum effects, namely persistent currents in a quantum ring threaded by a static magnetic field [16] and electron pumping under two periodically varying potentials with different phases [17], makes it possible to establish an electric current through connected double-ring systems [18,19]. The resulting current remains finite even if the two leads have identical chemical potentials and the system is in equilibrium. A key ingredient in the AB pump based on connected double-rings is the symmetry breaking due to the oscillating potentials with different phases. But pumping becomes impossible without the static

flux that yields persistent current [18]. In this context, Ramos et al. have considered a quantum ring with a quantum dot embedded in one of its arms [20]. A time-harmonic gate voltage was applied to the quantum dot. These authors have demonstrated that the inversion symmetry is not essential to pump electrons, provided that the quantum ring is threaded by a static magnetic flux.

Interference effects of coherent electrons open the possibility of controlling quantum transport without relying on potential barriers or magnetic flux [21,22]. In contrast to previous studies mentioned above on magnetically induced interference effects, in this work we consider a new design of quantum pump based on connected quantum rings, in which electron transport is controlled without applying a magnetic field. We demonstrate that pumped charge can be tuned by applying oscillating side-gate voltages across the rings instead. We show that in this case the phase shift between the two side-gate voltages breaks the symmetry and the system behaves as an efficient quantum pump. In other words, a net electric current is obtained even in equilibrium, and the magnitude of the current is controlled by the phase shift. The pumped current vanishes only for certain values of the phase shift or the chemical potential.

2. Coupled quantum rings under AC side-gate voltages

The system under consideration consists of two quantum rings connected in series and attached to two leads (source and drain). Side-gate voltages $V_{\pm}(t)$ break the symmetry of the upper and lower arms of the rings, as shown in Fig. 1, and act as additional parameters for controlling the electric current through the device, as recently suggested for graphene-based [21,22] and semiconductor nanorings [23]. We assume that the side-gate voltages can be

* Corresponding author.

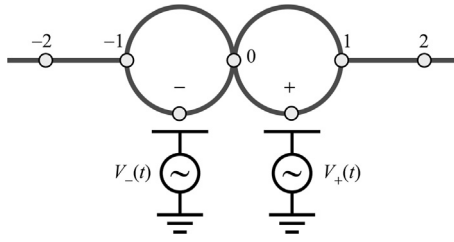


Fig. 1. Schematic diagram of the quantum rings subjected to side-gate voltages $V_{\pm}(t)$. The equivalent lattice model replaces the side-gate voltages by time-dependent site energies $\varepsilon_{\pm}(t)$ at sites labeled \pm and two other sites with index ± 1 are attached to semi-infinite chains.

modulated harmonically in time with frequency ω . We neglect capacitance effects as those described in Ref. [24] within the context of quantum rings threaded by an oscillating AB flux.

In order to study electron transport across the connected quantum rings, we mapped the system onto a much simpler yet non-trivial lattice model, depicted in Fig. 1. We replace each quantum ring by three sites of a lattice within the tight-binding approximation. One of the sites, labeled 0, is shared by the two quantum rings. Two sites, labeled \pm , have time-dependent energies $\varepsilon_{\pm}(t)$ and the other two sites, labeled ± 1 , are connected to semi-infinite chains. The time-dependent site energies are given by $\varepsilon_{\pm}(t) = V_0 \cos(\omega t \pm \phi)$, where 2ϕ is the phase shift between the two side-gate voltages. To avoid the profusion of free parameters, we assume a uniform transfer integral and vanishing site energies except at sites \pm , without loosing generality. The common value of the transfer integral will be set as the unit of energy and we take $\hbar = 1$ throughout the paper.

The time-dependent Schrödinger equation for the amplitude $\psi_j(t)$ at site j reads

$$i\dot{\psi}_j = \varepsilon_{\pm}(t)\delta_{j,\pm}\psi_j - \sum_{\ell(j)} \psi_{\ell(j)}, \quad (1)$$

where the index $\ell(j)$ runs over the neighboring sites of j and the dot indicates the derivative with respect to time. Using the Floquet formalism, the solution can be expressed in the form

$$\psi_j(t) = \sum_{n=-\infty}^{\infty} A_{n,j} e^{-iE_n t}, \quad (2a)$$

where $E_n = E + n\omega$, E being the quasienergy and n the sideband channel index. Since we are interested in electron transmission across the system, we take the following ansatz for the coefficients $A_{n,j}$ in the expansion (2a)

$$A_{n,j} = \begin{cases} \delta_{n0} e^{ik_n j} + r_n e^{-ik_n j}, & j \leq -1, \\ g_n^{\pm}, & j = \pm, \\ f_n, & j = 0, \\ t_n e^{ik_n j}, & j \geq 1. \end{cases} \quad (2b)$$

This solution corresponds to an electron propagating from the left to the right. Since the phase ϕ breaks the inversion symmetry of the system, the resulting transmission coefficient is not the same as that obtained for an electron coming from the right to the left. This broken symmetry will ultimately lead to the quantum pumping effect.

Inserting the ansatz (2) into the Schrödinger equation (1) yields

$$\begin{aligned} \delta_{n0} + r_n &= f_n + g_n^-, \\ E_n g_n^- - \alpha_- g_{n+1}^- - \alpha_+ g_{n-1}^- + f_n + \delta_{n0} e^{-ik_n} + r_n e^{ik_n} &= 0, \\ E_n f_n + \delta_{n0} e^{-ik_n} + r_n e^{ik_n} + t_n e^{ik_n} + g_n^+ + g_n^- &= 0, \\ E_n g_n^+ - \alpha_+ g_{n+1}^+ - \alpha_- g_{n-1}^+ + f_n + t_n e^{ik_n} &= 0, \\ t_n &= f_n + g_n^+, \end{aligned} \quad (3)$$

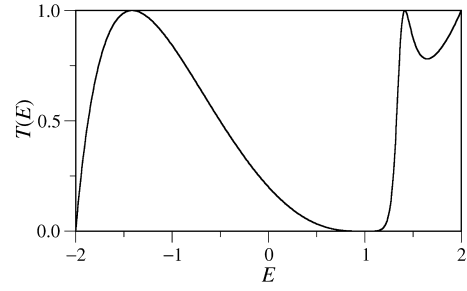


Fig. 2. Transmission probability as a function of energy at zero side-gate voltage. Transmission vanishes at $E = 1$ and displays two local maxima at $E = \pm\sqrt{2}$.

where for brevity we have defined $\alpha_{\pm} = (V_0/2)e^{\pm i\phi}$. After straightforward algebra one gets

$$\begin{aligned} [ie^{ik_n} \cot(k_n/2) - e^{-ik_n}] g_n^{\pm} - \alpha_{\pm} g_{n+1}^{\pm} - \alpha_{\mp} g_{n-1}^{\pm} \\ + ie^{ik_n} \cot(k_n/2) g_n^{\mp} = -1 - e^{\mp ik_n}. \end{aligned} \quad (4)$$

Once the amplitudes g_n^{\pm} have been calculated, the transmission amplitudes t_n are easily obtained with the help of (3). Finally, the transmission probability for the electron coming from the left is

$$T_{\rightarrow}(E, \omega, \phi) = \sum_n \frac{\sin k_n}{\sin k_0} |t_n|^2, \quad (5)$$

where the sum runs over the propagating channels, namely those channels for which $E_n = E + n\omega$ lies within the band of the leads.

The pumped current also depends on the transmission probability for an electron coming from the right, $T_{\leftarrow}(E, \omega, \phi)$. Due to the symmetry breaking caused by the side-gate voltages oscillating out of phase, $T_{\rightarrow}(E, \omega, \phi)$ and $T_{\leftarrow}(E, \omega, \phi)$ are different. It is a matter of simple algebra to demonstrate that the corresponding equations for an electron incoming from the right are similar to (3) but replacing $g_n^{\pm} \rightarrow g_n^{\mp}$ and $\alpha_{\pm} \rightarrow \alpha_{\mp}$. Finally, the pumped current density in equilibrium at zero temperatures is given by [18]

$$J(E_F, \omega, \phi) = \frac{2e}{h} \int_{-2}^{E_F} [T_{\rightarrow}(E, \omega, \phi) - T_{\leftarrow}(E, \omega, \phi)] dE, \quad (6)$$

where E_F is the Fermi energy and -2 is the minimum energy of the bands at the leads. The time-reversal symmetry is maximally broken when the side-gate voltages are in quadrature ($\phi = \pi/4$) and one would expect maximum pumping efficiency. We will show that this is indeed the case.

3. Results

3.1. Zero side-gate voltages

To gain insight into the transmission properties of the connected quantum rings, it is instructive to consider the time-independent case by setting $V_0 = 0$ for the moment. Under these circumstances, only the elastic channel is relevant and the transmission probability $T(E) = |t_0|^2$ can be easily computed with the aid of (3)

$$T(E) = \frac{(E+2)(E-1)^2}{2E^3 - 11E + 10}. \quad (7)$$

Fig. 2 shows the transmission probability as a function of the energy of the incoming electron at zero side-gate voltage. As seen in the figure, transmission vanishes at $E = 1$ and reaches unity at $E = \pm\sqrt{2}$ and at the upper band edge.

The vanishing of the transmission profile at $E = 1$ shown in Fig. 2 can be understood from the coupling of the local modes

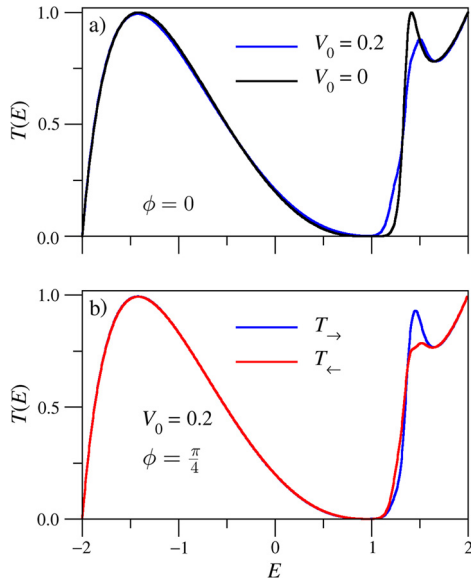


Fig. 3. (a) Transmission probability when $\omega = 0.1$, $V_0 = 0.2$ and $\phi = 0$ (blue line). In this case $T_{\rightarrow} = T_{\leftarrow}$. Results are compared with the transmission probability in the static case (black line). (b) Left and right transmission probabilities at $\omega = 0.1$ and $V_0 = 0.2$ when the side-gate voltages are in quadrature ($\phi = \pi/4$). (For interpretation of the references to color in this figure legend, the reader is referred to the web version of this article.)

of the two rings to the continuum of states at the leads. The Schrödinger equation (1) when the rings are not connected to the leads can be cast in the matrix form

$$\begin{pmatrix} 0 & -1 & -1 & 0 & 0 \\ -1 & 0 & -1 & 0 & 0 \\ -1 & -1 & 0 & -1 & -1 \\ 0 & 0 & -1 & 0 & -1 \\ 0 & 0 & -1 & -1 & 0 \end{pmatrix} \begin{pmatrix} \varphi_{-1} \\ \varphi_{-} \\ \varphi_0 \\ \varphi_{+} \\ \varphi_{+1} \end{pmatrix} = E \begin{pmatrix} \varphi_{-1} \\ \varphi_{-} \\ \varphi_0 \\ \varphi_{+} \\ \varphi_{+1} \end{pmatrix}, \quad (8)$$

where φ_j are the time-independent amplitudes at the five sites of the two isolated rings (see Fig. 1). Eq. (8) can be readily solved to obtain the corresponding eigenstates and eigenvalues. It is then found that there are two doubly degenerate eigenstates, namely $[1, -1, 0, 0, 0]^T$ and $[0, 0, 0, -1, 1]^T$, with energy $E = 1$. This energy is inside the bands of the leads and the corresponding probability amplitude vanishes at one of the rings. Therefore, at this energy the two leads are effectively decoupled and, consequently, transmission vanishes, in agreement with the results shown in Fig. 2. This is an example of the so-called bound states in the continuum. These exotic states reveal themselves as zeros of the transmission probability [23].

3.2. AC side-gate voltages

We now turn to our main goal, the occurrence of quantum pumping when the side-gate voltages depends harmonically on time. For that purpose we solved numerically the system of Eqs. (3) for three and five channels without significant changes in the results. When the driving frequency is not large, the transmission pattern is noticeably modified at quasienergies above $E = 1$ only, as clearly seen in Fig. 3(a) for $\omega = 0.1$, $V_0 = 0.2$ and $\phi = 0$. Results are compared with the transmission in the static case, shown in Fig. 1. The two connected rings are no longer perfectly transparent at $E = \sqrt{2}$ as in the static case. It is important to stress that $T_{\rightarrow} = T_{\leftarrow}$ when $\phi = 0$, as expected.

Left and right transmission probabilities are the same when $\phi = 0$ or $\phi = \pi/2$, namely when the phase shift between the two voltages vanishes or equals π . In this situation the pumped current

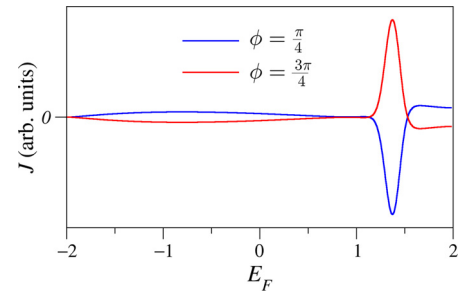


Fig. 4. Pumped current in arbitrary units as a function of the Fermi energy at $\omega = 0.1$ and $V_0 = 0.2$.

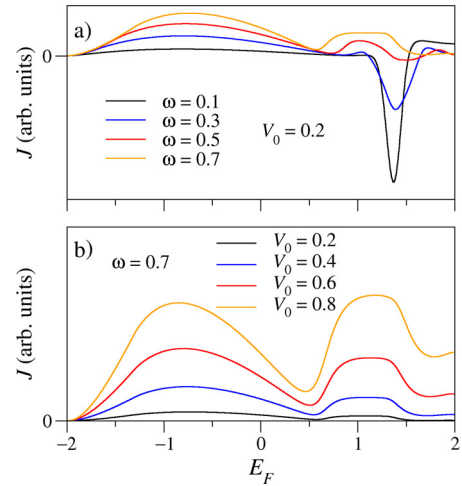


Fig. 5. Pumped current as a function of the Fermi energy when side-gate voltages are in quadrature ($\phi = \pi/4$). Different (a) frequencies and (b) side-gate voltages values, indicated on each plot, were considered.

vanishes. However, other values yield different left and right transmission probability, especially around the maximum at $E = \sqrt{2}$. Fig. 3(b) shows that at low frequency ($\omega = 0.1$) T_{\rightarrow} and T_{\leftarrow} are different when E is close to $\sqrt{2}$. Consequently, electron pumping is expected to occur in the system.

From Fig. 3 we are led to the conclusion that the pumped current at low frequency ($\omega = 0.1$) is small if $E_F < 1$ since in this range the right and left transmission probabilities are almost the same at the scale of the plot. This prediction proves to be correct, as seen in Fig. 4, where we plot the pumped current density in arbitrary units as a function of the Fermi energy, for the same parameters ω and V_0 as in Fig. 3. Notice the occurrence of the symmetry $J(E_F, \omega, \phi) = -J(E_F, \omega, \pi - \phi)$, which is nothing but the inversion of the electric current when the phase shift 2ϕ between the two side-gate voltages is reversed.

On increasing the frequency, the energy region below $E = 1$ starts to contribute to the pumped current and eventually both energy ranges (below and above $E = 1$) yield similar contributions. Fig. 5 shows dependence of the pumped current density on the various parameters of the model (frequency ω and side-gate voltage V_0) at $\phi = \pi/4$. The general trend is that the pumped current increases on increasing the frequency or the side-gate voltage over a wide range of Fermi energy.

4. Conclusions

In summary, we have considered a system consisting of two connected quantum rings subjected to side-gate voltages oscillating in time with frequency ω and studied its transport properties in a fully coherent regime. The use of the Floquet formalism allows us to obtain the pumped current in equilibrium, when the

chemical potentials of the leads are the same. The pumped current at zero temperature turns out to be nonzero except for specific values of the phase shift between the two side-gate voltages and Fermi energy. Although quantum pumps based on connected quantum rings have already been proposed in the literature [18,19], the origin of the pumping effect is different. Former proposals relied on the coexistence of persistent currents due to a static magnetic field and electron pumping under two periodically varying magnetic fluxes with different phases. On the contrary, in our proposal the pumped current is generated and controlled only by side-gated voltages. This new design seems to be more advantageous for real-world applications since no magnetic fields are needed and, consequently, it can be easily integrated in standard electronic circuits.

Acknowledgements

The authors thank J. Munárriz and P. Orellana for helpful discussions. R. P. A. L. would like to thank CAPES via project PPCP-Mercosul (grant number 25/2011), CNPq (Brazilian Research Agencies, project 472204/2010-6) and FAPEAL (Alagoas State Research Agency, project 2011.0908.011.0025.0087) for partial financial support. F. D-A. acknowledges support from MINECO (projects MAT2010-17180 and MAT2013-46308).

References

- [1] A. Lorke, R. Luyken, M. Fricke, J. Kotthaus, G. Medeiros-Ribeiro, J. Garcia, P. Petroff, *Microelectron. Eng.* 47 (1999) 95.
- [2] A. Lorke, R. Johannes Luyken, A.O. Govorov, J.P. Kotthaus, J.M. Garcia, P.M. Petroff, *Phys. Rev. Lett.* 84 (2000) 2223.
- [3] R.J. Warburton, C. Schaflein, D. Haft, F. Bickel, A. Lorke, K. Karrai, J.M. Garcia, W. Schoenfeld, *Nature* 405 (2000) 926.
- [4] E. Ribeiro, A.O. Govorov, W. Carvalho, G. Medeiros-Ribeiro, *Phys. Rev. Lett.* 92 (2004) 126402.
- [5] M. Bayer, O. Stern, P. Hawrylak, S. Fafard, *Nature* 405 (2000) 923.
- [6] M. Bayer, M. Korkusinski, P. Hawrylak, T. Gutbrod, M. Michel, A. Forchel, *Phys. Rev. Lett.* 90 (2003) 186801.
- [7] F. Ding, N. Akopian, B. Li, U. Perinetti, A. Govorov, F.M. Peeters, C.C. Bof Bufon, C. Deneke, Y.H. Chen, A. Rastelli, O.G. Schmidt, V. Zwiller, *Phys. Rev. B* 82 (2010) 075309.
- [8] T. Ihn, A. Fuhrer, M. Sigrist, K. Ensslin, W. Wegscheider, M. Bichler, in: B. Kramer (Ed.), *Advances in Solid State Physics*, vol. 43, Springer, Berlin, Heidelberg, 2003, pp. 139–154.
- [9] Y. Aharonov, D. Bohm, *Phys. Rev.* 115 (1959) 485.
- [10] R.G. Chambers, *Phys. Rev. Lett.* 5 (1960) 3.
- [11] R.A. Römer, M.E. Raikh, *Phys. Rev. B* 62 (2000) 7045.
- [12] A.O. Govorov, S.E. Ulloa, K. Karrai, R.J. Warburton, *Phys. Rev. B* 66 (2002) 081309.
- [13] K. Mouloupoulos, M. Constantinou, *Phys. Rev. B* 70 (2004) 235327.
- [14] M.D. Teodoro, V.L. Campo, V. Lopez-Richard, E. Marega, G.E. Maraga, Y.G. Gobato, F. Iikawa, M.J.S.P. Brasil, Z.Y. AbuWaar, V.G. Dorogan, Y.I. Mazur, M. Benamara, G.J. Salama, *Phys. Rev. Lett.* 104 (2010) 086401.
- [15] C. González-Santander, F. Domínguez-Adame, R.A. Römer, *Phys. Rev. B* 84 (2011) 235103.
- [16] R. Landauer, M. Büttiker, *Phys. Rev. Lett.* 54 (1985) 2049.
- [17] P.W. Brouwer, *Phys. Rev. B* 58 (1998) R10135.
- [18] D. Shin, J. Hong, *Phys. Rev. B* 70 (2004) 073301.
- [19] D. Shin, J. Hong, *Phys. Rev. B* 72 (2005) 113307.
- [20] J.P. Ramos, L.E.F. Foa-Torres, P.A. Orellana, V.M. Apel, *J. Appl. Phys.* 115 (2014) 124507.
- [21] J. Munárriz, F. Domínguez-Adame, A.V. Malyshev, *Nanotechnology* 22 (2011) 365201.
- [22] J. Munárriz, F. Domínguez-Adame, P.A. Orellana, A.V. Malyshev, *Nanotechnology* 23 (2012) 205202.
- [23] C. González-Santander, P.A. Orellana, F. Domínguez-Adame, *Europhys. Lett.* 102 (2013) 17012.
- [24] M. Büttiker, *Phys. Scr. T* 54 (1994) 104.